International Journal of the Physical Sciences Vol. 8(7), pp. 277-285, 23 February, 2013
Available online at http://www.academicjournals.org/IJPS
DOI: 10.5897/IJPS2013.3839
ISSN 1992 - 1950 ©2013 Academic Journals

Full Length Research Paper

Aftershock sequence analysis of 19 May, 2009 earthquake of Lunayyir lava flow, northwest Saudi Arabia

Al-Zahrani H.[1]*, Al-Amri A. M.[1, 3], Abdel-Rahman K.[1, 2] and Fnais M.[1]

[1]Department of Geology and Geophysics, King Saud University, Riyadh, Saudi Arabia.
[2]Department of Seismology, National Research Institute of Astronomy and Geophysics, Cairo, Egypt.
[3]Water Resources Exploration Chair In the Empty Quarter, King Saud University, Riyadh, Saudi Arabia.

Accepted 19 February, 2013

Aftershock sequence of 19th May, 2009 Lunayyir earthquake (Mw 5.7) has been recorded by deploying seismic stations immediately after the occurrence of the main shock. Analysis of this sequence clarified that; the major part of cumulative seismic moment released during the first hours after the occurrence of the main shock; their orientation is north west (NW) parallel to the Red Sea axial trend along Najd faulting system; it is clustered at two depths; from 5-10 and 15-25 km beneath Lunayyir area; illustrated successive periods of maxima and minima; decayed rapidly following the relation of n(t)=37.28 t-0.6. Fault plane solutions for five large events indicate normal faulting is the major mechanism. These findings are in agreement with the north east (NE) (transform fault) trend runs crossing the Red Sea into Shield area where the activity has been initiated and travelled through the Lunayyir area. While the NW Najd faulting system runs parallel to the Red Sea axial trend and intersected with NE fault trend underlying Lunayyir area. Accordingly, it can be concluded that, the recent earthquake activities at Lunayyir lava flow area are related to the present-day Red Sea tectonics. Monitoring earthquake activities through installing permanent seismic network around the area is highly recommended.

Key words: aftershock sequence, fault plane solution, stress, and Lunayyir.

INTRODUCTION

Lunayyir lava flow area lies between Latitudes 25°.10 - 25°.17 N and Longitudes 37°.45 - 37°.75 E in the northwestern part of Saudi Arabia (Figure 1). It is oriented, generally, northwest-southeast (Laurent and Chevrel, 1980) parallel to the Red Sea axial trend. It has been experienced in October 2007 an earthquake swarm with maximum magnitude of 3.2, while in 2009 another earthquake swarm has been initiated on 19th April and increased gradually till its maximum on 19th of May where the main shock (M_w 5.7) was occurred. Great number of aftershocks with maximum magnitude of 4.8 was recorded. This earthquake activity was close to some scattered urban communities (for example, Al Ays town, 40 km southeast of the epicenter). Accordingly, Saudi government evacuated more than 40,000 people (Pallister et al., 2010).

Field survey has been done for the epicentral area immediately after the mainshock occurrence (Fnais, 2010; Jónsson et al., 2010; Al-Zahrani, 2010). Depending on these investigations, there are crakes with different directions while the total length of surface rupture was extended up to 8 km and 90 cm of offset with the main shock (Fukao and Kikushi, 1987). It is known that the stress drop on the fault plane due to the occurrence of an earthquake produces an increase of effective shear stress around the rupture area (Chinnery, 1963). The transferring in the static stress may explain the location of some aftershocks away from the fault.

GEOLOGICAL AND TECTONIC SETTING

Lunayyir lave flow area imposed in the Shield area that composed of hard rocks and surficial soft sediments

*Corresponding author. E-mail: alzaharani.h@hotmail.com.

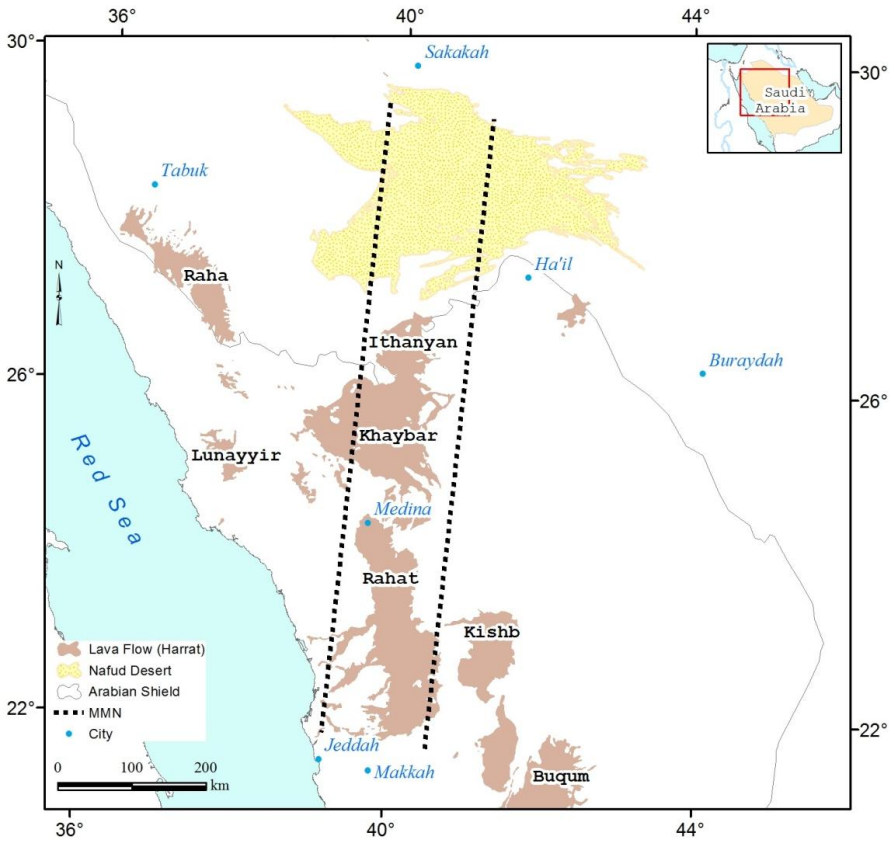

Figure 1. Location of Lunayyir Lava flow.

ranges in age from precambrian to recent. Precambrian rocks represented by gneisses and schists that had been subjected to strong folding and faulting. Tertiary to Holocene basalts composed of alkaline olivine basalt, whereas quaternary sediments extend along some Wades in the northern part of the area.

Tectonically, Lunayyir area was subjected to two episodes of tectonic movements synchronized with the Red Sea floor spreading through pre-early Miocene rifting period (Girdler, 1969; Anon, 1972; Rose et al., 1973). It has been controlled-to great extent-by the regional stress regime of the western Arabian plate associated with the Cenozoic development of the Red Sea. Harrat Lunayyir probably faulted during Cenozoic rift time where the up arching period was parallel to the Red Sea coast. During Late Miocene-Pliocene, the alkali basalt invaded into the Harrat Lunayyir. According to the above-mentioned, there are different fault trends prevailing the area and oriented NE-SW, NNW-SSE, and NW-SE (Figure 2).

RECORDING OF AFTERSHOCK SEQUENCE

King AbdulAziz City for Science and Technology (KACST) and King Saud University (KSU) installed two sub-networks of seismic stations at the epicentral area on 20th May for recording the aftershock sequence (Figures 3 and 4, and Table 1).

KACST sub-network consists of 15 short-period seismic stations and one of broadband, while KSU sub-network composed of 6 stations of short period with the same configuration of KACST stations. Each of the short period stations is equipped by short period SS-1 seismometer (Kinemetrics Inc.); Quantira digitizer as seismic data logger (Q_{330}) and Baler (20GB hard disk) for storing of recorded earthquakes; and 12-volt battery and solar panel for continuous charging, while, broadband station include broadband Streckeisen STS-2 seismometer (Kinemetrics Inc.). The data has been collected with sampling rate of 300 SPS for the broadband and short period as well.

First arrival times of P and S-waves were picked to compute the hypocentral parameters using modified HYPO71PC software version (Lee and Valdes, 1985). Furthermore, some of recorded data was analyzed using HYPOINVERSE software (Klein, 1987) which calculates the standard errors of hypocentral parameters as well. Two of 1-D velocity models (Makris et al., 1978; Al-Amri et al., 2008) have been used through data processing in this study. Residual values from crustal models were compared with no significant differences have been

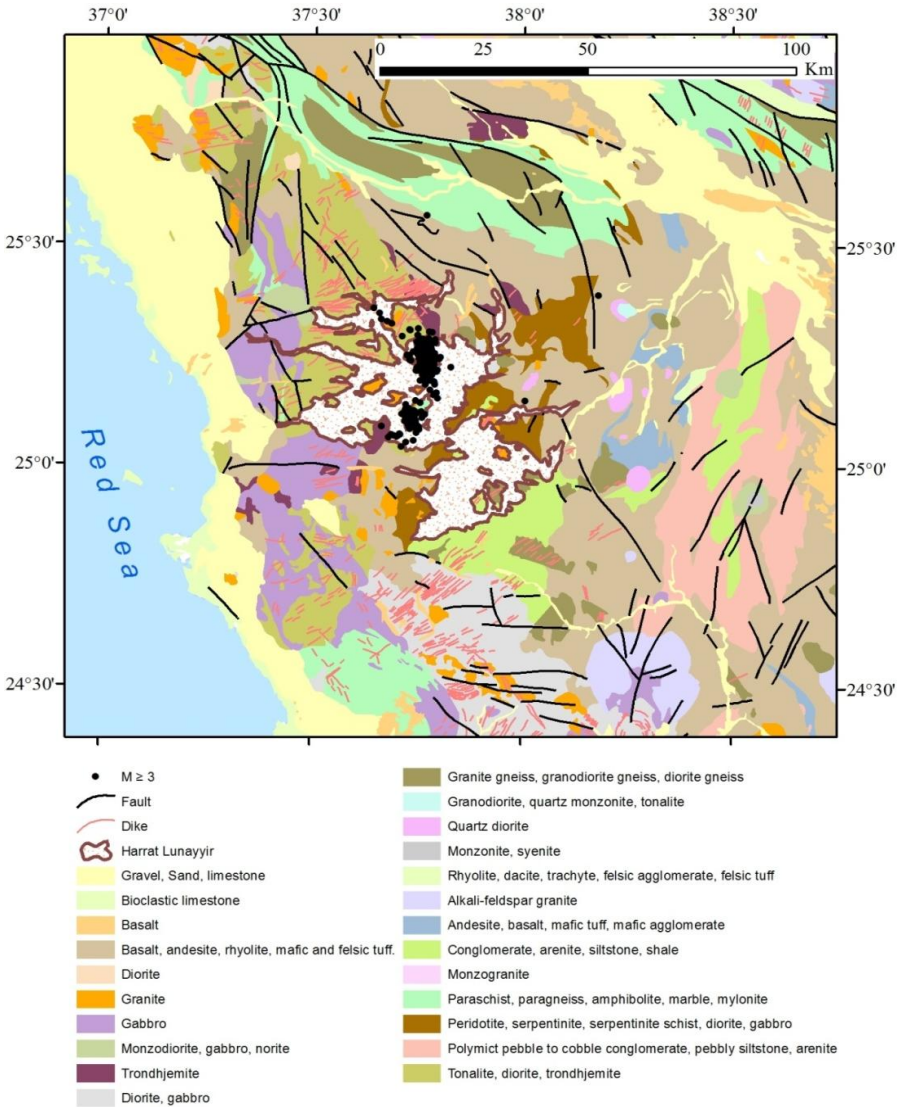

Figure 2. Geological setting around Lunayyir area.

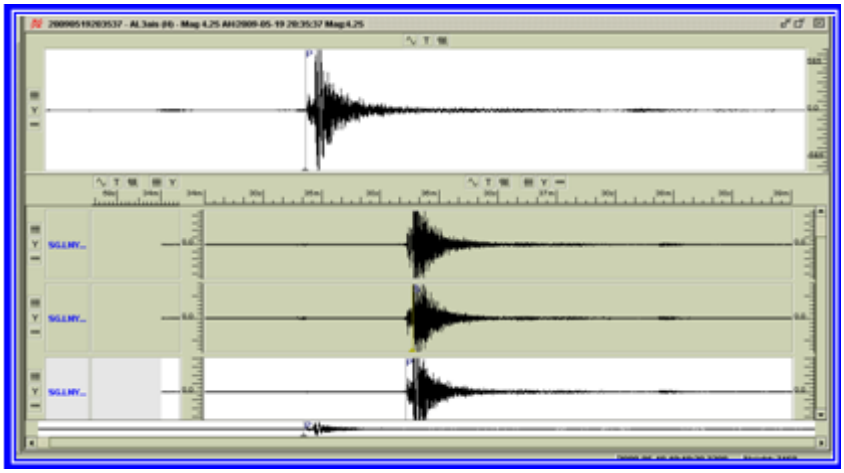

Figure 3. Waveform of 2009-05-19 aftershock (20:35:37 and M = 4.25).

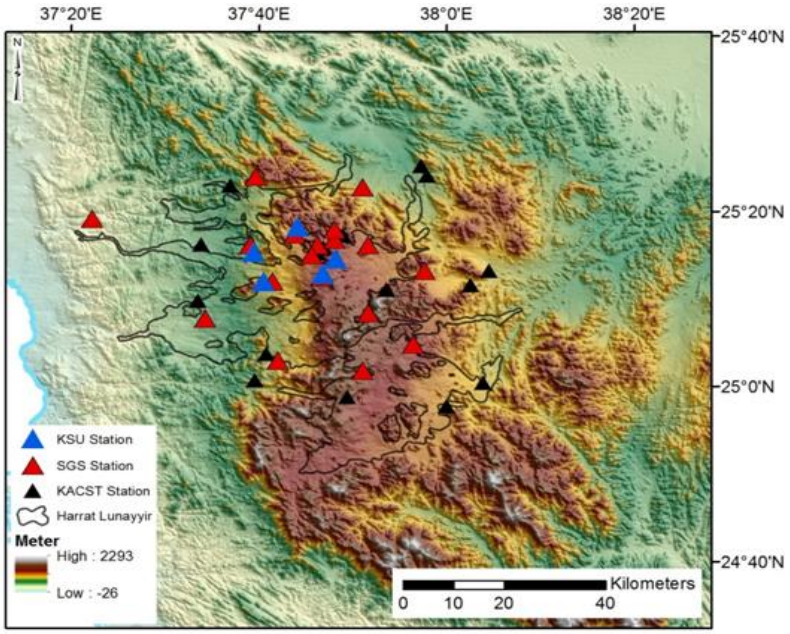

Figure 4. Map of two seismic deployments (KSU and KACST).

Table 1. Parameters of KACST and KSU sub-networks at Lunnayyir area.

Station code	Latitude (N)	Longitude (E)	Elevation (m)	Seismometer	Data logger
STN01	25.2554	37.7698	1010	STS-2	Q_{330}
STN02	25.0618	37.6792	559	SS-1	Q_{330}
STN03	25.1851	37.8929	946	SS-1	Q_{330}
STN04	25.2640	37.7805	970	SS-1	Q_{330}
STN05	25.1637	37.5574	393	SS-1	Q_{330}
STN06	25.1934	38.0424	600	SS-1	Q_{330}
STN07	25.4015	37.9651	600	SS-1	Q_{330}
STN08	25.3823	37.6161	600	SS-1	Q_{330}
STN09	24.9631	37.9994	600	SS-1	Q_{330}
STN10	25.0120	37.6592	600	SS-1	Q_{330}
STN11	25.2877	37.8155	956	SS-1	Q_{330}
STN12	25.2708	37.5637	600	SS-1	Q_{330}
STN13	25.0072	38.0650	600	SS-1	Q_{330}
STN14	24.9802	37.8231	600	SS-1	Q_{330}
STN15	25.2204	38.0755	600	SS-1	Q_{330}
STN16	25.4202	37.9542	600	SS-1	Q_{330}
KSU01	25.2134	37.7794	1011	SS-1	Q_{330}
KSU02	25.2423	37.8026	957	SS-1	Q_{330}
KSU03	25.3030	37.7355	962	SS-1	Q_{330}
KSU04	25.2555	37.6571	551	SS-1	Q_{330}
KSU05	25.1989	37.6743	551	SS-1	Q_{330}

noticed between HYPO71 and HYOINVERSE programs, where the epicentral difference was less than 0.5 km. whereas the depths, which more sensitive to the velocity model, differed by about 1 km on average. Consequently, the hypocentral parameters given by HYPO71 were quite realistic.

Accordingly, 1050 of well-located aftershocks during the period of observation (20th May till 20th June) have

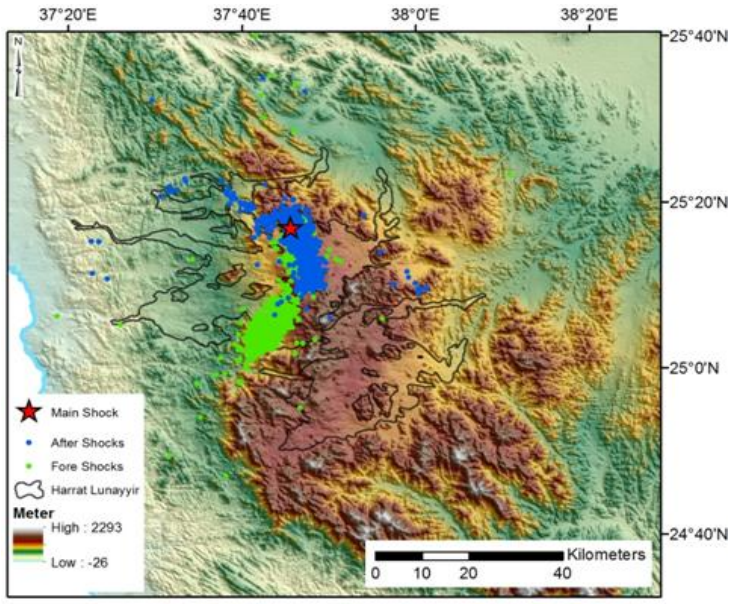

Figure 5. Aftershock sequence from 20 May - 19 June.

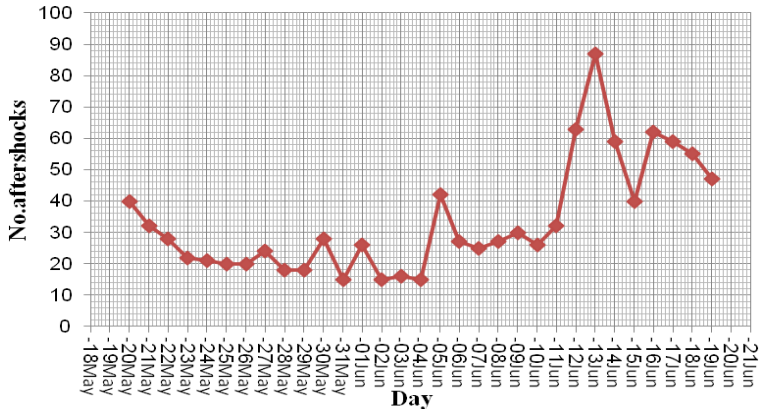

Figure 6. Relationship between numbers of aftershocks per day.

been analyzed through this study (Figure 5). Depending on Figure 5 aftershocks are extend northeast at the beginning and changed later into northwest. Figure 6 illustrates three episodes of maxima as follows; from 29th May - 2nd June; from 4th - 6th June; and from 11th - 13th June. These episodes were overlapped by three episodes of minima. These aftershocks are of crustal origin where it is clustered at two depth intervals between 5 to 10 km and from 15 to 25 km (Figure 7).

RATE OF DECAY FOR AFTERSHOCKS SEQUENCE

It is indicated that, the occurrence rate of aftershocks, N(t) obeys the modified Omori relation (Kisslinger, 1997; Gheitanchi, 2003; Benito et al., 2004). The empirical relation for the rate of decay estimation has been suggested by Omori (Utsu, 1961). This relation combine the frequency of aftershocks N(t) per unit time t, following the main shock and represented by:

$$N(t) = k/t^{-c}$$

Where K and c are constants and should be estimated for each region.

More than 400 well-located aftershocks (M ≥ 2.0) have been used to estimate the rate of decay for Lunayyir earthquake swarm. The cyclic activation of aftershocks was indicated by their heterogeneities. Hence, first month of aftershock observation could be differentiated into

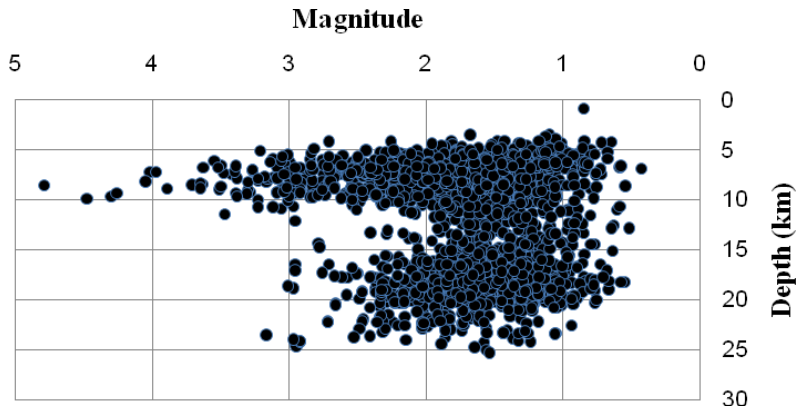

Figure 7. Magnitude – Depth relationship.

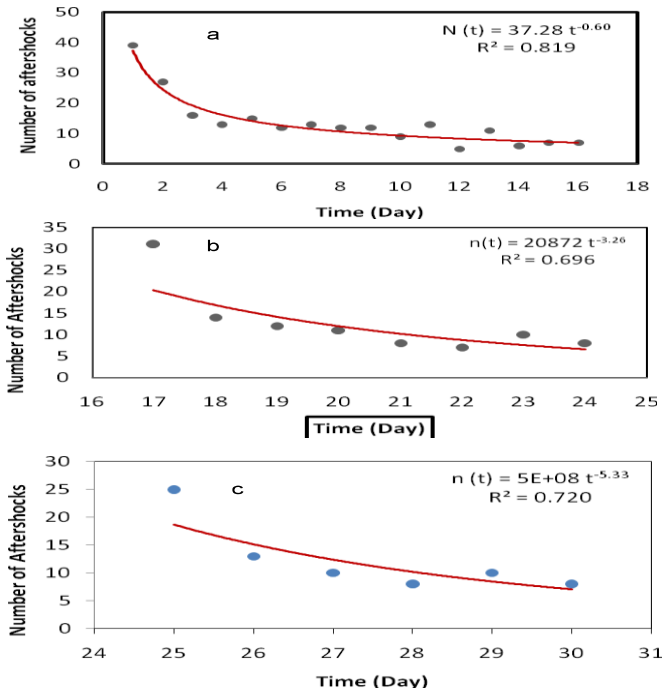

Figure 8. Rate of decay for the aftershock sequence (M ≥ 2).

three intervals; the first interval from 20th May till 4th June; the second from 5th-12th June, while the third from 13th - 19th June (Figure 8) as follows:

N (t) = 37.28 $t^{-0.60}$, with R^2 = 0.82 (for the first two weeks),
N (t) = 20872 $t^{-3.26}$, with R^2 = 0.7 (for the third week), and
N (t) = 5E+08 $t^{-5.33}$, with R^2 = 0.72 (for the last week)

Where N (t) being the number of events by day, t is the time in days after the main shock, and R^2 is the correlation coefficient. Figure 8 indicates that, there are three different rates of decay through the first month of observation for the aftershocks of M ≥ 2.0. Another noticeable feature for Lunayyir aftershock sequence is the releasing of major part of the cumulative seismic moment during the first hours after the main shock. Excluding the first day (20th May, 2009), no event with local magnitude above 4.0 was recorded during the period of recording.

FOCAL MECHANISM

The first motion polarities of P-wave have been picked for the large earthquakes (M ≥ 4.0) to estimate the fault plane solution for these aftershocks using the PMAN program (Suetsugu, 2003). The input parameters of the azimuths and take-off angles were calculated based on

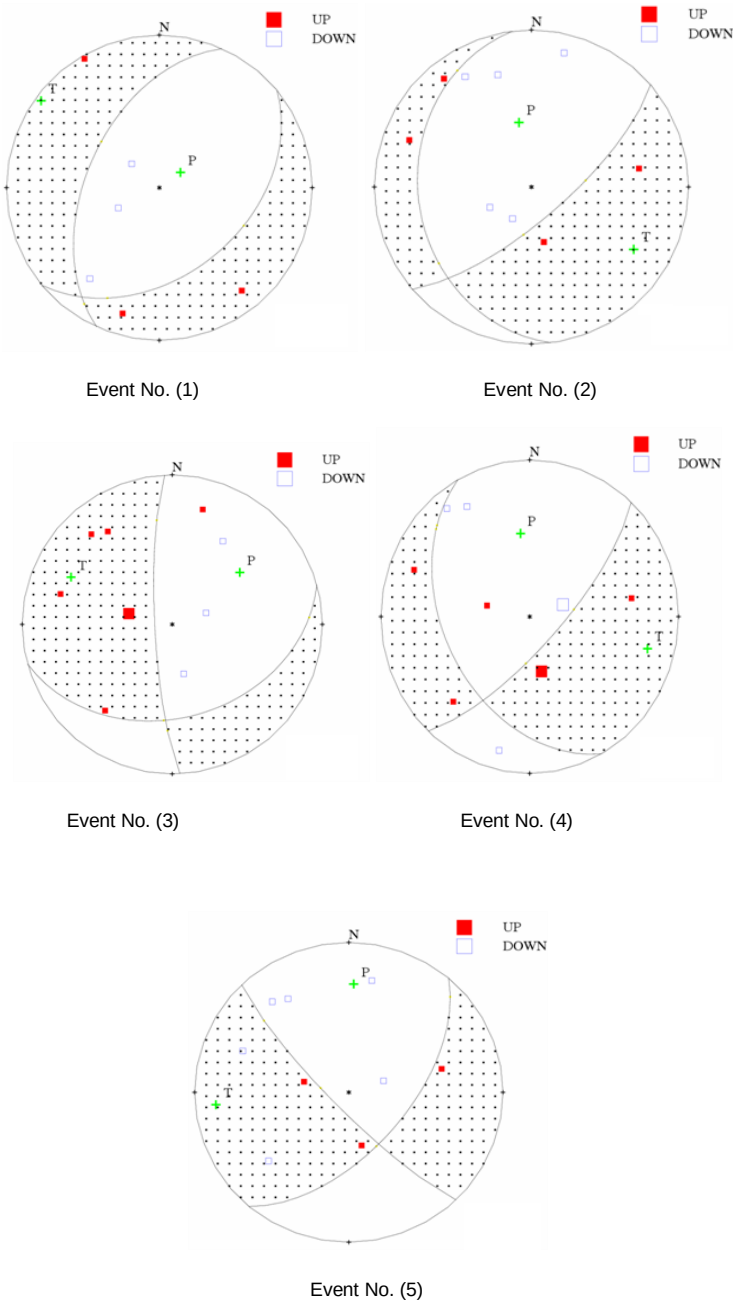

Figure 9. Fault plane solution for large aftershocks.

1-D velocity model of Al-Amri et al. (2008). Figure 9 shows fault plane mechanisms of large aftershocks by equal area projections of the lower focal hemisphere while their parameters are listed in Tables 2 and 3.

DISCUSSION

The recorded aftershocks are oriented NW parallel to the Red Sea axial trend. Furthermore, the focal mechanism of the large aftershocks illustrated NW trend is the main faulting trend of normal mechanism. The extensional stress (*T*-axis) is directed NE, while NW trend represents the compressional stress (*P*-axis). These results are in agreement with the field measurements for the ground cracks and fissures accompanied with the main shock (Jónsson et al., 2010; Fnais, 2010). These aftershocks are of crustal origin where it is clustered at two depths of 5 to 10 km and 15 to 25 km beneath Lunayyir area. By considering the depth of the main shock was 9 km, it indicates that the rupture process was initiated at depth of 9 km and propagated with bilateral behavior of

Table 2. Source parameters for aftershocks used for focal plane solutions.

Event No.	Nodal Plane 1			Nodal Plane 1			P-axis		T-axis	
	Strike (°)	Dip (°)	Rake (°)	Strike (°)	Dip (°)	Rake (°)	Pl. (°)	Az. (°)	Pl. (°)	Az. (°)
1	204	51	-107	50	42	-70	76	54	4	-54
2	173	28	-143	49	73	-67	56	349	25	121
3	177	81	-127	75	38	-16	43	52	26	-65
4	43	74	-50	151	42	-156	46	353	19	104
5	136	81	-149	40	59	-11	28	3	14	-95

Table 3. Fault plane mechanism for large aftershocks.

Event No.	Date			Origin time			Location		Depth (Km)	Mag.
	y	m	d	H	M	S	Lat. (°N)	Long. (°E)		
1	2009	05	19	18	20	00	25.2820	37.7665	9.62	4.29
2	2009	05	19	19	21	27	25.2885	37.7622	7.20	4.01
3	2009	05	19	19	26	58	25.2733	37.7653	8.23	4.04
4	2009	05	19	20	35	37	25.3093	37.7303	9.30	4.25
5	2009	05	20	19	57	16	25.2975	37.7505	8.49	4.79

directivity. Aftershock sequence was represented by overlapping cycles of maxima and minima with different numbers and magnitudes. This may reflect the non-homogeneity in stress levels owing to the different episodes of magmatic dyke intrusions (Al-Amri and Fnais, 2009; Zahran et al., 2009). Most of the accumulated energy was released shortly after the main shock and decreased rapidly with different rates of decay which may be explains the presence of small scale ground cracks and fissures intersected with the major ruptures at the epicentral area (Mukhopadhyay et al., 2012; Al-Zahrani et al., 2012).

These results clarified the affecting of Lunayyir area with the present-day active tectonics related to the Red Sea floor spreading. Accordingly, the continuous monitoring for the volcano-tectonic activities and earthquake hazards at Lunayyir lava flow area are highly recommended.

ACKNOWLEDGEMENT

This project was supported by King Saud University, Deanship of Scientific Research, College of Science Research Center.

REFERENCES

Al-Amri A, Fnais M (2009). Seismo-volcanic investigation of 2009 earthquake swarms at Harrat Lunayyir (Ash Shaqah), Western Saudi Arabia. Int. J. Earth Sci. Eng. India (in press).

Al-Amri A, Rodgers A, Al-khalifah T (2008). Improving the Level of Seismic Hazard Parameter in Saudi Arabia Using Earthquake Location. Arabian J. Geosci. 1:1-15 DOI 10.1007/s12517-008-0001-5.

Al-Zahrani H (2010). An Investigation of Seismo-volcanic Sources of Harrat Lunayyir, NW Al-Madinah Al- Munawwarah. M.Sc. Thesis, Fac. Sci., King Saud Univ., 102 P.

Al-Zahrani H, Fnais M, Al-Amri A, Abdel-Rahman K (2012). Tectonic framework of Lunayyir area, northwest Saudi Arabia through aftershock sequence analysis of 19 May, 2009 earthquake and aeromagnetic data. Int. J. Phys. Sci. 7(44):5821-5833.

Anon (1972). The Sea that is really an ocean. New Scientist 34:414-445.

Benito B, Cepeda J, Martinez Diaz J (2004). Analysis of the spatial and temporal distribution of the 2001 earthquakes in El Savador, in Rose, W.I., Bommer, J.J., Lopez, D.L., Carr, M.J., and Major, J.J, eds., Natural hazards in El Salvador: Boulder, Colorado. Geol. Soc. Am. special paper 375:1-18.

Chinnery M (1963). The stress changes that accompany strike-slip faulting. Bull. Seismol. Soc. Am. 53:921-932.

Fnais M (2010). Coseismic Ruptures caused by 19 May 2009 Earthquake (M_w 5.7), Western Saudi Arabia. Bull. Egypt Geophys. Soc. (in press).

Fukao Y, Kikuchi M (1987). Source retrieval for mantle earthquakes by iterative deconvolution of long-period P-waves. Tectonophysics 144:249-269.

Gheitanch M (2003). Analysis of the 1990 Fork (Darab), southern Iran, earthquake sequence. J. Earth Space Phys. 29(1):13-19.

Girdler R (1969). The Red Sea-a geophysical background. In: Degens ET, Ross D. A. (eds): Hot brines and recent heavy metal deposits in the Red Sea. Springer, New York pp. 59-70.

Jónsson S, Pallister J, McCausland W, El-Hadidy S (2010). Dyke Intrusion and Arrest in Harrat Lunayyir, western Saudi Arabia, in April - July 2009. Geophys. Res. 12, EGU2010-7704.

Kisslinger C (1997). Aftershocks and fault zone properties. Adv. Geophys. 38:1-35.

Klein RW (1987). Hypocenter location program. HYPOINVERSE, part 1: user guide, open file report. U.S .Geological Survey, Menlo Park, California 113 pp.

Laurent D, Chevrel S (1980). Prospecting for Pozzolan on Harrat Lunayyir. Ministry of Petrol and Mineral Resources.

Lee W, Valdes C (1985). HYPO71PC: A personal computer version of the HYPO71 earthquake location program. U.S .Geological Survey Open File Report 85-749, 43 pp.

Makris J, Allam A, Mokhtar T, Basahel A, Dehghani, Bazari (1978). Crustal structure of northeast region of Saudi Arabia and its transition

to the Red Sea. Internal Report, National Research Institute of Astronomy and Geophysics, Egypt.
Mukhopadhyay, B, Mogren S, Mukhopadhyay M, Dasgupta S (2012). Incipient status of dyke intrusion in top crust – evidences from the Al-Ays 2009 earthquake swarm, Harrat Lunayyir, SW Saudi Arabia. Geo. Nat. Hazards Risk. 1:1-19.
Pallister J, McCausland W, Jónsson S, Lu Z, Zahran H, El-Hadidy S, Aburukbah A, Stewart I, Lundgern P, White R, Moufti M (2010). Broad accommodation of rift-related extension recorded by dyke intrusion in Saudi Arabia. Nat. Geosci. 8 pp.
Rose D, Whitmarsh R, Ali S, Boudreaux J, Coleman R, Fleisher R, Girdler R, Manheim F, Matter A, Nigrini C, Stoffers P, Supko P (1973). Red Sea, Drilling. Science. 179:377-380.
Suetsugu D (2003). PMAN The program for focal mechanism diagram with p-wave polarity data using the equal-area projection. IISEE Lecture Note, Tsukuba, Japan pp. 44-58.
Utsu T (1961). A statistical study on the occurrence of aftershocks. Geophys. Mag. 30:521-605.
Zahran H, McCausland W, Pallister J, Lu Z, El-Hadidy S, Aburukba A, Schawali J, Kadi K, Youssef A, Ewert J, White R, Lundgren P, Mufti M, Stewart I (2009). Stalled eruption or dike intrusion at Harrat Lunayyir, Saudi Arabia?. Am. Geophys. Union, abstract, V13E-2072.